

Fully heavy asymmetric scalar tetraquarks

S. S. Agaev,¹ K. Azizi,^{2,3,*} and H. Sundu⁴

¹*Institute for Physical Problems, Baku State University, Az-1148 Baku, Azerbaijan*

²*Department of Physics, University of Tehran, North Karegar Avenue, Tehran 14395-547, Iran*

³*Department of Physics, Doğuş University, Dudullu-Ümraniye, 34775 Istanbul, Türkiye*

⁴*Department of Physics Engineering, Istanbul Medeniyet University, 34700 Istanbul, Türkiye*

(ΩDated: December 23, 2024)

The scalar tetraquarks T_b and T_c with asymmetric contents $bb\bar{b}\bar{c}$ and $cc\bar{c}\bar{b}$ are explored using the QCD sum rule method. These states are modeled as the diquark-antidiquarks composed of the axial-vector components. The masses and current couplings of T_b and T_c are calculated using the two-point sum rule approach. The predictions obtained for the masses of these four-quark mesons prove that they are unstable against the strong two-meson fall-apart decays to conventional mesons. In the case of the tetraquark T_b this is the decay $T_b \rightarrow \eta_b B_c^-$. The processes $T_c \rightarrow \eta_c B_c^+$ and $J/\psi B_c^{*+}$ are kinematically allowed decay modes of the tetraquark T_c . The widths of corresponding processes are evaluated by employing the QCD three-point sum rule approach which are necessary to estimate strong couplings at the tetraquark-meson-meson vertices of interest. The mass $m = (15697 \pm 95)$ MeV and width $\Gamma[T_b] = (36.0 \pm 10.2)$ MeV of the tetraquark T_b as well as the parameters $\tilde{m} = (9680 \pm 102)$ MeV and $\Gamma[T_c] = (54.7 \pm 9.9)$ MeV in the case of T_c provide useful information to search for and interpret new exotic states.

I. INTRODUCTION

Fully heavy tetraquarks, i.e., four-quark exotic mesons containing exclusively heavy b and c quarks were and remain interesting objects for theoretical investigations. Related problems were explored in numerous publications aimed to calculate the masses of such hadrons, investigate their stability against strong interactions and find kinematically allowed decay channels. These studies permitted one to collect valuable information about features of these hypothetical hadrons existence of which, nevertheless, is not forbidden by laws of the parton model and quantum chromodynamics. Researchers also elaborated new theoretical models and methods to investigate these exotic hadrons.

Recently, the LHCb-ATLAS-CMS collaborations discovered four scalar X resonances presumably with $cc\bar{c}\bar{c}$ contents [1–3]. This observation gave strong impetus to physics of fully-heavy tetraquarks and placed it on the strong foundation of experimental data. This achievement generated also new theoretical works to interpret X resonances as diquark-antidiquark states or hadronic molecules, and explain their measured parameters (see, Refs. [4–7] and references therein). In our articles, we computed the masses and widths of the different models for the X structures [4–7]. We found that some of them may be considered as ground-level or radially excited diquark-antidiquark states, whereas others probably are hadronic molecules or superpositions of these two structures.

There are numerous fully heavy tetraquarks with interesting contents and properties. The particles $bb\bar{c}\bar{c}$ are very intriguing objects for studies, because they carry two

units of electric charge. They also may really be strong-interaction stable structures. The reason is that their contents exclude creation of conventional mesons via the annihilation of internal heavy quark-antiquark pairs originally studied in Refs. [8, 9]. Therefore, $bb\bar{c}\bar{c}$ may be stable particles provided their masses are smaller than the corresponding $B_c B_c$ meson thresholds. Our studies, however, demonstrated that the masses of the tetraquarks $bb\bar{c}\bar{c}$ with quantum numbers $J^P = 0^\pm, 1^\pm$ and 2^+ are above the relevant limits and they are relatively wide compounds [10–12].

Another class of fully heavy four-quark mesons is a family of hidden charm-bottom particles $bc\bar{b}\bar{c}$. The structures $bc\bar{b}\bar{c}$ were not discovered yet, but have real chances to be seen in ongoing and future experiments [13, 14]. Properties of these tetraquarks were studied in numerous publications by employing different methods and models [15–23]. They were considered also in our articles [24–26], in which we calculated the masses and widths of the scalar, axial-vector and tensor particles. Let us note that the full widths of these tetraquarks were evaluated by taking into account the fall-apart processes and decays triggered by $b\bar{b}$ annihilation inside of the exotic mesons. It turned out that these tetraquarks are relatively wide structures with widths around of 100 MeV.

Apart from the tetraquarks discussed above there are particles with asymmetric contents, i.e., particles composed of unequal number of b and c quarks $bb\bar{b}\bar{c}$ or $cc\bar{c}\bar{b}$. They also attracted interests of researches and were explored in a number of publications [17, 27–31], where the authors used various approaches ranging from a potential till the relativistic quarks models. The predictions obtained in these articles also differ from each other. The main parameter calculated there is the mass of $bb\bar{b}\bar{c}$ or $cc\bar{c}\bar{b}$ states with different spin-parities: Decays of these tetraquarks, as usual, were not explored quantitatively. Therefore, there is a necessity to perform comprehensive

*Corresponding Author

analysis of the asymmetric fully heavy four-quark systems by including their decay modes.

In the current article, we investigate the scalar tetraquarks $bb\bar{b}\bar{c}$ or $cc\bar{c}\bar{b}$ and, in what follows, label them as T_b and T_c , respectively. We treat these particles as the diquark-antidiquark compounds built of the axial-vector diquark and antidiquark. We apply the two-point QCD sum rule method [32, 33] to compute the masses and current couplings of these structures. Our predictions for the masses of T_b and T_c demonstrate that they are unstable against strong dissociations to two conventional mesons. In the case of T_b this is the decay $T_b \rightarrow \eta_b B_c^-$. The processes $T_c \rightarrow \eta_c B_c^+$ and $J/\psi B_c^{*+}$ are kinematically allowed fall-apart decays in the case of T_c . To evaluate partial widths of these modes, we employ the three-point sum rule approach, which is required to evaluate the strong couplings of tetraquarks T_b and T_c and final conventional mesons.

This paper is structured in the following way: In Sec. II, we compute the spectroscopic parameters of the scalar diquark-antidiquark states T_b and T_c . The widths of the decay $T_b \rightarrow \eta_b B_c^-$ is calculated in Sec. III. The full width of the tetraquark T_c saturated by the channels $T_c \rightarrow \eta_c B_c^+$ and $J/\psi B_c^{*+}$ is evaluated in section IV. We make our conclusions in the last part of the article V.

II. SPECTROSCOPIC PARAMETERS OF THE TETRAQUARKS T_b AND T_c

Here, we concentrate on the masses and current couplings of the diquark-antidiquark states T_b and T_c in the context of QCD two-point sum rule approach. In this method one has to introduce interpolating currents for the structures T_b and T_c and calculate relevant correlation functions. In its turn, the interpolating currents are determined by the internal organizations of the tetraquarks, i.e., by the spin-parities of the constituent diquarks and antidiquarks.

Here, we are going to explain this question in the case of the scalar structure $bb\bar{b}\bar{c}$: The same analysis is valid for the exotic meson $cc\bar{c}\bar{b}$ as well. In general, the scalar tetraquark T_b can be composed of five different diquarks without derivatives [34]. We restrict ourselves by considering the structure T_b which is made of the axial-vector ingredients. In this case T_b contains the diquark $b^T C \gamma_\mu b$ and antidiquark $\bar{b} \gamma^\mu C \bar{c}^T$. This information is necessary but not enough to fix unambiguously the interpolating current $J(x)$. The reason is that one also needs to reveal the color structure of the tetraquarks's components. The axial-vector diquark $q^T C \gamma_\mu q'$ may belong to the following flavor-color representations $(\mathbf{6}_f, \mathbf{\bar{3}}_c)$ and $(\mathbf{\bar{3}}_f, \mathbf{6}_c)$. It is evident that the diquark $b^T C \gamma_\mu b$ is flavor-symmetric state and $(\mathbf{6}_f, \mathbf{\bar{3}}_c)$ is the unique choice for the diquark. Then the antidiquark $\bar{b} \gamma^\mu C \bar{c}^T$ should have a structure $(\mathbf{\bar{6}}_f, \mathbf{3}_c)$ to form flavor-color singlet state. As a result, we get

$$J(x) = b_a^T(x) C \gamma_\mu b_b(x) [\bar{b}_a(x) \gamma^\mu C \bar{c}_b^T(x) - \bar{b}_b(x) \gamma^\mu C \bar{c}_a^T(x)], \quad (1)$$

where C is the charge conjugation matrix, and a and b are the color indices. This current describes the diquark-antidiquark state in $[\mathbf{\bar{3}}_c] \otimes [\mathbf{3}_c]$ representation of the color group.

One of alternative options for T_b may be a structure built of the scalar diquark $b^T C \gamma_5 b$ and antidiquark $\bar{b} \gamma_5 C \bar{c}^T$. But $b^T C \gamma_5 b$ is a member of the representation $(\mathbf{6}_f, \mathbf{6}_c)$, as a result, such current would correspond to the color-symmetric $[\mathbf{6}_c] \otimes [\mathbf{\bar{6}}_c]$ tetraquark which is less favorable than the antisymmetric ones [35].

The scalar particle $T_c = cc\bar{c}\bar{b}$ is constructed in analogous way and has the interpolating current

$$\tilde{J}(x) = c_a^T(x) C \gamma_\mu c_b(x) [\bar{c}_a(x) \gamma^\mu C \bar{b}_b^T(x) - \bar{c}_b(x) \gamma^\mu C \bar{b}_a^T(x)], \quad (2)$$

A. The mass and current coupling of the scalar state $bb\bar{b}\bar{c}$

We are going to derive the expressions for the mass m and current coupling Λ of the tetraquark T_b in the context of the QCD sum rule method [32, 33]. It is one of the powerful nonperturbative methods to extract parameters of the hadrons. Originally, it was proposed to study conventional particles, but is successfully used also to explore multiquark systems [36, 37].

We start our investigations from the correlation function

$$\Pi(p) = i \int d^4 x e^{ipx} \langle 0 | \mathcal{T} \{ J(x) J^\dagger(0) \} | 0 \rangle, \quad (3)$$

where \mathcal{T} is the time-ordered product of two currents. In accordance with SR method, the correlation function $\Pi(p)$ should be expressed by utilizing the physical parameters of the tetraquark m and Λ , and computed in the operator product expansion (OPE) with fixed accuracy by employing heavy quark propagators. The first expression forms the phenomenological side $\Pi^{\text{Phys.}}(p)$ of the SR equality, whereas the second one $\Pi^{\text{OPE}}(p)$ —its QCD side. Afterwards, by matching these two expressions within the hadron-quark duality assumption, and carrying out the manipulations explained below, one finds required SRs.

The correlator $\Pi^{\text{Phys.}}(p)$ is given by the expression

$$\Pi^{\text{Phys.}}(p) = \frac{\langle 0 | J | T_b \rangle \langle T_b | J^\dagger | 0 \rangle}{m^2 - p^2} + \dots, \quad (4)$$

which is the sum of the ground-level particle's contribution shown explicitly, and higher resonances and continuum states denoted by the ellipses.

We rewrite $\Pi^{\text{Phys}}(p)$ by utilizing the matrix element

$$\langle 0|J|T_b\rangle = \Lambda, \quad (5)$$

and get

$$\Pi^{\text{Phys}}(p) = \frac{\Lambda^2}{m^2 - p^2} + \dots \quad (6)$$

The term $\Lambda^2/(m^2 - p^2)$ in the right-hand side of Eq. (6) has the trivial Lorentz structure proportional to \mathbf{I} , and is the invariant amplitude $\Pi^{\text{Phys}}(p^2)$ required for future studies.

Alternatively, $\Pi^{\text{Phys}}(p^2)$ can be expressed through dispersion integral in terms of the spectral density $\rho^{\text{Phys}}(s)$

$$\rho^{\text{Phys}}(s) = \frac{1}{\pi} \text{Im}\Pi^{\text{Phys}}(s) = \Lambda^2 \delta(s - m^2) + \rho^{\text{h}}(s), \quad (7)$$

with $\Lambda^2 \delta(s - m^2)$ being the pole term, whereas $\rho^{\text{h}}(s)$ is unknown hadronic spectral density. Then, it is evident that

$$\Pi^{\text{Phys}}(p^2) = \frac{\Lambda^2}{m^2 - p^2} + \int_{\mathcal{M}^2}^{\infty} \frac{\rho^{\text{h}}(s) ds}{s - p^2}, \quad (8)$$

where $\mathcal{M}^2 = (3m_b + m_c)^2$.

At next phase of studies, we insert the current $J(x)$ into Eq. (3) and contract relevant quark fields to find $\Pi^{\text{OPE}}(p)$, which reads

$$\begin{aligned} \Pi^{\text{OPE}}(p) = & 2i \int d^4x e^{ipx} \text{Tr} \left[S_b^{b'a}(-x) \gamma_\mu \tilde{S}_c^{a'b}(-x) \gamma_\nu \right] \\ & \times \left\{ \text{Tr} \left[\gamma^\nu \tilde{S}_b^{aa'}(x) \gamma^\mu S_b^{bb'}(x) \right] + \text{Tr} \left[\gamma^\nu \tilde{S}_b^{bb'}(x) \gamma^\mu S_b^{aa'}(x) \right] \right. \\ & \left. - \text{Tr} \left[\gamma^\nu \tilde{S}_b^{ba'}(x) \gamma^\mu S_b^{ab'}(x) \right] - \text{Tr} \left[\gamma^\nu \tilde{S}_b^{ab'}(x) \gamma^\mu S_b^{ba'}(x) \right] \right\} \end{aligned} \quad (9)$$

where

$$\tilde{S}_{b(c)}(x) = CS_{b(c)}^T(x)C. \quad (10)$$

Here, $S_{b(c)}(x)$ are b and c quarks' propagators [37].

The amplitude $\Pi^{\text{OPE}}(p^2)$ is calculated in deep Euclidean region $p^2 \ll 0$ where coefficient functions in OPE is obtained using the perturbative QCD, whereas non-perturbative information is contained in the gluon condensates. Having continued $\Pi^{\text{OPE}}(p^2)$ analytically to the Minkowski domain and found its imaginary part, we get the two-point spectral density $\rho^{\text{OPE}}(s)$. In the region $p^2 \ll 0$ we apply the Borel transformation \mathcal{B} to remove subtraction terms in the dispersion integral and suppress contributions of higher resonances and continuum states. For $\mathcal{B}\Pi^{\text{Phys}}(p^2)$, we obtain

$$\mathcal{B}\Pi^{\text{Phys}}(p^2) = \Lambda^2 e^{-m^2/M^2} + \int_{\mathcal{M}^2}^{\infty} ds \rho^{\text{h}}(s) e^{-s/M^2}, \quad (11)$$

where M^2 is the Borel parameter. One can write the dispersion representation for the amplitude $\Pi^{\text{OPE}}(p^2)$ using

$\rho^{\text{OPE}}(s)$ as well. Then, by equating the Borel transformations of $\Pi^{\text{Phys}}(p^2)$ and $\Pi^{\text{OPE}}(p^2)$ and applying the assumption about hadron-parton duality $\rho^{\text{h}}(s) \simeq \rho^{\text{OPE}}(s)$ in a duality region, we subtract second term in Eq. (11) from the QCD side of the obtained equality and get

$$\Lambda^2 e^{-m^2/M^2} = \Pi(M^2, s_0). \quad (12)$$

Here,

$$\Pi(M^2, s_0) = \int_{\mathcal{M}^2}^{s_0} ds \rho^{\text{OPE}}(s) e^{-s/M^2} + \Pi(M^2), \quad (13)$$

where s_0 is the continuum subtraction parameter. The nonperturbative function $\Pi(M^2)$ is computed directly from the correlator $\Pi^{\text{OPE}}(p)$ and contains contributions that do not enter to the spectral density. The SRs for m and Λ of the state T_b can be extracted after computing the correlation function $\Pi(p)$ using both the physical parameters of T_b and heavy quark propagators. The first function $\Pi^{\text{Phys}}(p)$ establishes the phenomenological side of the sum rule, whereas $\Pi^{\text{OPE}}(p)$ constitutes its QCD side.

After simple manipulations, we get

$$m^2 = \frac{\Pi'(M^2, s_0)}{\Pi(M^2, s_0)}, \quad (14)$$

and

$$\Lambda^2 = e^{m^2/M^2} \Pi(M^2, s_0), \quad (15)$$

which are the sum rules for m and Λ , respectively. In Eq. (14), we also use $\Pi'(M^2, s_0) = d\Pi(M^2, s_0)/d(-1/M^2)$. The spectral density $\rho^{\text{OPE}}(s)$ contains the perturbative $\rho^{\text{pert.}}(s)$ and nonperturbative $\rho^{\text{Dim}^4}(s)$ terms. We do not provide the explicit formulas for the functions $\rho^{\text{OPE}}(s)$ and $\Pi(M^2)$, because they are rather lengthy.

We need to specify the input parameters in Eqs. (14) and (15) to perform numerical computations. Some of them are universal quantities: The masses of b and c quarks and gluon vacuum condensate $\langle \alpha_s G^2/\pi \rangle$ are such parameters. In present work, we use following values

$$\begin{aligned} m_b &= 4.18_{-0.02}^{+0.03} \text{ GeV}, \quad m_c = (1.27 \pm 0.02) \text{ GeV}, \\ \langle \alpha_s G^2/\pi \rangle &= (0.012 \pm 0.004) \text{ GeV}^4. \end{aligned} \quad (16)$$

The m_b and m_c are the running quark masses in the $\overline{\text{MS}}$ scheme [38]. The gluon vacuum condensate was extracted from analysis of various hadronic processes in Refs. [32, 33].

Contrary, the Borel and continuum subtraction parameters M^2 and s_0 are specific for each problem and should satisfy some standard constraints of SR computations. Dominance of the pole contribution (PC) in extracted quantities and their stability upon variations of M^2 and s_0 as well as convergence of the operator product expansion are important conditions for correct SR analysis. To fulfill these requirements, we impose on the parameters

M^2 and s_0 the following restrictions. First, the pole contribution

$$\text{PC} = \frac{\Pi(M^2, s_0)}{\Pi(M^2, \infty)}, \quad (17)$$

should obey $\text{PC} \geq 0.5$. The convergence of OPE is second important condition in the SR analysis. Because, the correlation function contains only nonperturbative dimension-4 term $\Pi^{\text{Dim4}}(M^2, s_0)$, we require fulfilment of the constraint $|\Pi^{\text{Dim4}}(M^2, s_0)| = 0.05\Pi(M^2, s_0)$, which ensures the convergence of the operator product expansion. It is worth noting that the maximum of the Borel parameter is determined from Eq. (17), whereas convergence of OPE allows us to fix its minimal value.

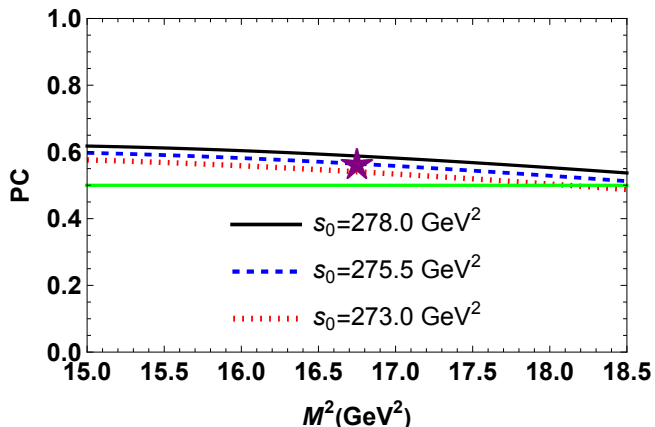


FIG. 1: Dependence of PC on the Borel parameter M^2 at fixed s_0 . The red star shows the point $M^2 = 16.75 \text{ GeV}^2$ and $s_0 = 275.5 \text{ GeV}^2$.

Numerical calculations are performed over a wide range of the parameters M^2 and s_0 . Analysis of these

predictions allows us to fix the working windows for M^2 and s_0 , where all aforementioned restrictions are obeyed. We find that the regions

$$M^2 \in [15, 18.5] \text{ GeV}^2, \quad s_0 \in [273, 278] \text{ GeV}^2, \quad (18)$$

comply with these constraints. Indeed, on the average in s_0 at maximal and minimal M^2 the pole contribution is $\text{PC} \approx 0.51$ and $\text{PC} \approx 0.6$, respectively. The nonperturbative term is positive and at $M^2 = 15 \text{ GeV}^2$ forms less than 1% of the whole result. The dependence of PC on the Borel parameter is shown in Fig. 1, in which all curves exceed the limit line $\text{PC} = 0.5$.

To extract m and Λ , we compute their mean values over the regions Eq. (18) and find

$$\begin{aligned} m &= (15698 \pm 95) \text{ MeV}, \\ \Lambda &= (9.30 \pm 1.03) \text{ GeV}^5. \end{aligned} \quad (19)$$

Effectively, results in Eq. (19) are equal to SR predictions at the point $M^2 = 16.75 \text{ GeV}^2$ and $s_0 = 275.5 \text{ GeV}^2$, where $\text{PC} \approx 0.56$, which ensures the dominance of PC in the extracted parameters. Uncertainties in Eq. (19) are generated mainly by the choices of M^2 and s_0 . These theoretical errors form only $\pm 0.6\%$ of the mass m , which demonstrates the high stability of the obtained prediction. Such accuracy of the result is connected with the SR for m Eq. (14) which determines it as a ratio of the correlation functions. Therefore, changes in the correlators due to M^2 , s_0 compensate in m each other and stabilize by this way the numerical output. In the case of Λ errors are amount to $\pm 11\%$ of the central value, but still remain within limits acceptable of the sum rule analysis. In Fig. 2, we show m as a function of M^2 and s_0 .

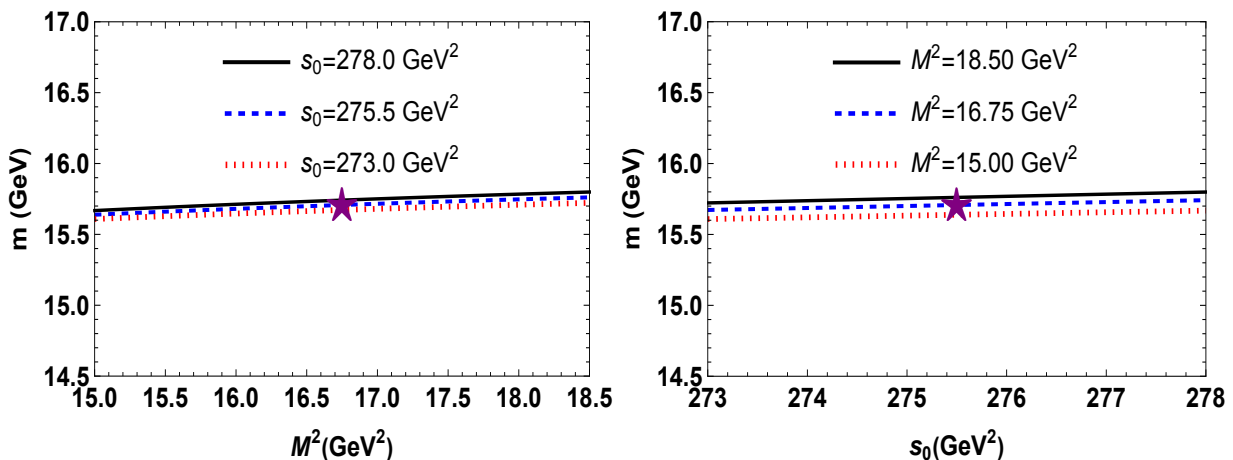


FIG. 2: The mass m as a function of the Borel M^2 (left panel), and continuum threshold s_0 parameters (right panel).

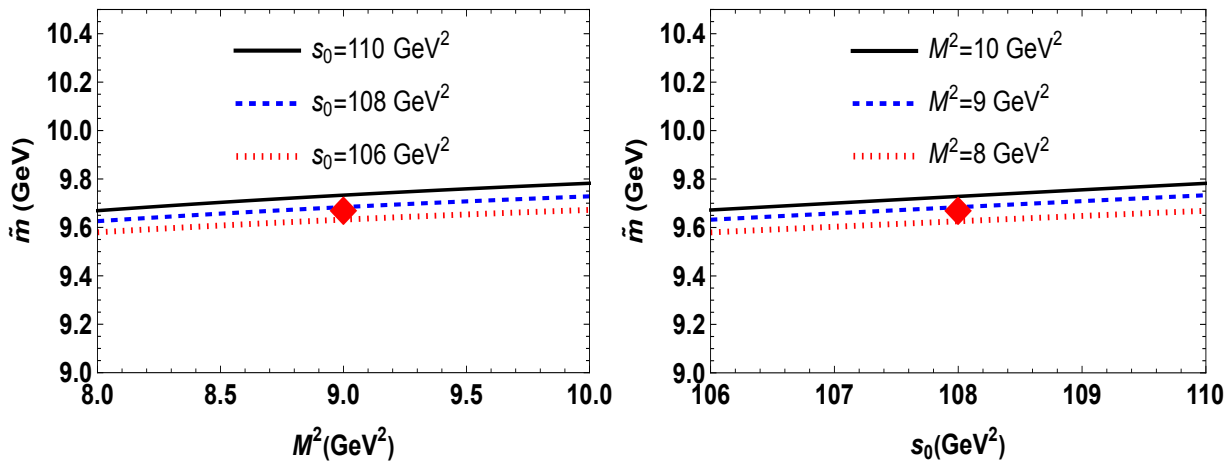


FIG. 3: Dependence of \tilde{m} on the Borel M^2 (left panel), and continuum threshold s_0 parameters (right panel). The red diamond is placed at $M^2 = 9$ GeV² and $s_0 = 108$ GeV².

B. Parameters of the tetraquark T_c

The expressions for the correlation functions $\tilde{\Pi}^{\text{Phys}}(p)$ and $\tilde{\Pi}^{\text{OPE}}(p)$, as well as the SRs for \tilde{m} and $\tilde{\Lambda}$ in the case of the tetraquark T_c with content $cc\bar{c}\bar{b}$ differ from ones obtained in the subsection by replacements $m_b \leftrightarrow m_c$. Therefore, we omit related details and write down only the working intervals for the auxiliary parameters M^2 and s_0 . Numerical computations prove that

$$M^2 \in [8, 10] \text{ GeV}^2, \quad s_0 \in [106, 110] \text{ GeV}^2, \quad (20)$$

comply with all necessary constraints. Really, on the average in s_0 at maximal $M^2 = 10$ GeV² the pole contribution is $\text{PC} \approx 0.50$, whereas at $M^2 = 8$ GeV² it is equal to $\text{PC} \approx 0.73$. The nonperturbative term is positive and at $M^2 = 8$ GeV² forms 0.4% of the whole result.

To extract \tilde{m} and $\tilde{\Lambda}$, we compute their average values over the regions Eq. (20) and find

$$\begin{aligned} \tilde{m} &= (9680 \pm 102) \text{ MeV}, \\ \tilde{\Lambda} &= (1.55 \pm 0.22) \text{ GeV}^5. \end{aligned} \quad (21)$$

Dependence of the mass \tilde{m} on the Borel parameter M^2 and s_0 is depicted in Fig. 3.

The diquark-antidiquark states $bb\bar{b}\bar{c}$ and $cc\bar{c}\bar{b}$ with different spin-parities were investigated in various articles [17, 27–31]. It is interesting to compare our findings with predictions for the mass of the scalar tetraquarks made in these works. Thus, in Ref. [17] the authors used the nonrelativistic quark model where the Hamiltonian contains the linear confining and Coulomb potentials and spin-spin interactions. The results for the mass of the tetraquarks $bb\bar{b}\bar{c}$ composed of the color-triplet and color-sextet diquarks were found equal to 16158 MeV and 16173 MeV, respectively. In this paper, the mass of the scalar states $cc\bar{c}\bar{b}$ were estimated as 9740 MeV and 9763 MeV.

Three different models, i.e., the color-magnetic interaction model, the constituent quark and multiquark flux-tube models were used in Ref. [27] to evaluate the mass of the tetraquarks under consideration. The authors considered the superpositions of the states built of color-triplet and -sextet diquarks. For the mass of the scalar $bb\bar{b}\bar{c}$ the color-magnetic interaction model predicted 15713 MeV, whereas the constituent quark model led to the result 16175 MeV. As is seen, there is an approximately 300 MeV mass gap between two models. The same is true in the case of the tetraquark $cc\bar{c}\bar{b}$ as well: 9314 MeV and 9753 MeV, respectively.

The dynamical diquark and the relativistic diquark-antidiquark models [29, 31] gave 16060 MeV and 16102 MeV, respectively. For the tetraquark $cc\bar{c}\bar{b}$ the authors found 9579 MeV and 9606 MeV. Let us note that these predictions corresponds to pure $[\mathbf{3}_c] \otimes [\mathbf{3}_c]$ diquark-antidiquark states. In these articles one can also find very detailed information on the various theoretical results about the masses of the particles $bb\bar{b}\bar{c}$ and $cc\bar{c}\bar{b}$.

Comparing our SR predictions $m = 15698$ MeV and $\tilde{m} = 9680$ MeV with ones obtained in the context of the different quark models, we see that the mass of the T_b state is compatible with prediction of the color-magnetic interaction model [27] and is considerably smaller than results of other works. Contrary, the mass \tilde{m} of the tetraquark T_c , in some cases, exceeds predictions of the alternative models. It is interesting to note that the difference $(3m_b + m_c) - (m_b + 3m_c) = 5820$ MeV is close to $m - \tilde{m} \approx 6000$ MeV which is 300–400 MeV smaller than the corresponding mass gaps in the quark models.

III. DECAY $T_b \rightarrow \eta_b B_c^-$

Information on the mass of the tensor state T_b allows us to fix its decay channels. The decay to $\eta_b B_c^-$ mesons

is kinematically possible process for the transformation of the tetraquark T_b to ordinary mesons. The mesons η_b and B_c^- have the masses $m_{\eta_b} = (9398.7 \pm 2.0)$ MeV and $m_{B_c} = (6274.47 \pm 0.27 \pm 0.17)$ MeV [38], respectively. As a result, the threshold 15673 MeV for creation of the final state $\eta_b B_c^-$ is below m .

The width of the decay $T_b \rightarrow \eta_b B_c^-$, besides the usual input parameters is determined by the strong coupling G at the vertex $T_b \rightarrow \eta_b B_c^-$. It can be calculated by employing the form factor $G(q^2)$ at the mass shell $q^2 = m_{B_c}^2$. In its turn, the form factor $G(q^2)$ can be extracted from analysis of the correlation function

$$\begin{aligned} \Pi(p, p') &= i^2 \int d^4x d^4y e^{ip'y} e^{-ipx} \langle 0 | \mathcal{T} \{ J^{\eta_b}(y) \\ &\quad \times J^{B_c^-}(0) J^\dagger(x) \} | 0 \rangle, \end{aligned} \quad (22)$$

where $J^{\eta_b}(x)$ and $J^{B_c^-}(x)$ are interpolating currents of the pseudoscalar mesons η_b and B_c^- , respectively

$$J^{\eta_b}(x) = \bar{b}_i(x) i \gamma_5 b_i(x), \quad J^{B_c^-}(x) = \bar{c}_j(x) i \gamma_5 b_j(x). \quad (23)$$

Here, i and j are the color indices.

To find the physical side of the sum rule $\Pi^{\text{Phys}}(p, p')$, we have to write Eq. (22) using parameters of the particles T_b , η_b and B_c^- . To this end, we recast the correlator $\Pi(p, p')$ into the form

$$\begin{aligned} \Pi^{\text{Phys}}(p, p') &= \frac{\langle 0 | J^{\eta_b} | \eta_b(p') \rangle \langle 0 | J^{B_c^-} | B_c^-(q) \rangle}{p'^2 - m_{\eta_b}^2} \frac{\langle 0 | J^{B_c^-} | B_c^-(q) \rangle}{q^2 - m_{B_c}^2} \\ &\quad \times \langle \eta_b(p') B_c^-(q) | T_b(p) \rangle \frac{\langle T_b(p) | J^\dagger | 0 \rangle}{p^2 - m^2} + \dots, \end{aligned} \quad (24)$$

where we have presented explicitly only the contribution of the ground-level particles, whereas effects due to higher resonances and continuum states are denoted by the dots.

The Eq. (24) can be further detailed using the matrix elements of the mesons η_b and B_c^-

$$\begin{aligned} \langle 0 | J^{\eta_b} | \eta_b(p') \rangle &= \frac{f_{\eta_b} m_{\eta_b}^2}{2m_b}, \\ \langle 0 | J^{B_c^-} | B_c^-(q) \rangle &= \frac{f_{B_c} m_{B_c}^2}{m_b + m_c}. \end{aligned} \quad (25)$$

In (25) $f_{\eta_b} = 724$ MeV and $f_{B_c} = (371 \pm 37)$ MeV are decay constants of the mesons [39]. Besides, we have to specify the vertex $\langle \eta_b(p') B_c^-(q) | T_b(p) \rangle$, which in the case of the three spin-0 particles has a simply form

$$\langle \eta_b(p') B_c^-(q) | T_b(p) \rangle = G(q^2) p \cdot p'. \quad (26)$$

Then, we find for $\Pi^{\text{Phys}}(p, p')$

$$\begin{aligned} \Pi^{\text{Phys}}(p, p') &= \frac{G(q^2) \Lambda f_{\eta_b} m_{\eta_b}^2 f_{B_c} m_{B_c}^2}{2m_b(m_b + m_c)(p^2 - m^2)(p'^2 - m_{\eta_b}^2)} \\ &\quad \times \frac{1}{(q^2 - m_{B_c}^2)} \frac{m^2 + m_{\eta_b}^2 - q^2}{2} + \dots. \end{aligned} \quad (27)$$

The right hand side of this expression is the invariant amplitude $\Pi_0^{\text{Phys}}(p^2, p'^2, q^2)$ which will be utilized to derive the sum rule for the form factor $G(q^2)$.

For the QCD side of the sum rule, we get

$$\begin{aligned} \Pi^{\text{OPE}}(p, p') &= 2 \int d^4x d^4y e^{ip'y} e^{-ipx} \left\{ \text{Tr} \left[\gamma_5 S_b^{ja}(y-x) \right. \right. \\ &\quad \times \gamma_\mu \tilde{S}_b^{ib}(-x) \gamma_5 \tilde{S}_c^{ai}(x) \gamma^\mu S_b^{bj}(x-y) \left. \right] \\ &\quad \left. - \text{Tr} \left[\gamma_5 S_b^{ja}(y-x) \gamma_\mu \tilde{S}_b^{ib}(-x) \gamma_5 \tilde{S}_c^{bi}(x) \gamma^\mu S_b^{aj}(x-y) \right] \right\}. \end{aligned} \quad (28)$$

The correlator $\Pi^{\text{OPE}}(p, p')$ is equal to the amplitude $\Pi_0^{\text{OPE}}(p^2, p'^2, q^2)$. After simple manipulations, we find SR for $G(q^2)$

$$\begin{aligned} G(q^2) &= \frac{4m_b(m_b + m_c)(q^2 - m_{B_c}^2)}{\Lambda f_{\eta_b} m_{\eta_b}^2 f_{B_c} m_{B_c}^2 (m^2 + m_{\eta_b}^2 - q^2)} \\ &\quad \times e^{m^2/M_1^2} e^{m_{\eta_b}^2/M_2^2} \Pi_0(\mathbf{M}^2, \mathbf{s}_0, q^2). \end{aligned} \quad (29)$$

In Eq. (29), the function $\Pi_0(\mathbf{M}^2, \mathbf{s}_0, q^2)$ is $\Pi_0^{\text{OPE}}(p^2, p'^2, q^2)$ after Borel transformations and continuum subtractions. It depends on the parameters $\mathbf{M}^2 = (M_1^2, M_2^2)$ and $\mathbf{s}_0 = (s_0, s'_0)$ where the pairs (M_1^2, s_0) and (M_2^2, s'_0) correspond to T_b and η_b channels, respectively.

Constraints imposed on the auxiliary parameters \mathbf{M}^2 and \mathbf{s}_0 are universal for all SR computations and have been explained in the previous section. Numerical analysis shows that the regions in Eq. (18) for the parameters (M_1^2, s_0) and

$$M_2^2 \in [9, 11] \text{ GeV}^2, \quad s'_0 \in [95, 99] \text{ GeV}^2. \quad (30)$$

for (M_2^2, s'_0) satisfy all these requirements. Because, the form factor $G(q^2)$ depends on the mass and current coupling of the tetraquark T_b , this choice for (M_1^2, s_0) excludes also additional uncertainties in m and Λ , as well as in $G(q^2)$ which may appear beyond the regions Eq. (18).

The SR method leads to reliable predictions for the form factor $G(q^2)$ in the Euclidean region $q^2 < 0$. But $G(q^2)$ determines the strong coupling G at the mass shell $q^2 = m_{B_c}^2$. Therefore, it is convenient to introduce the function $G(Q^2)$ with $Q^2 = -q^2$ and use it in our analysis. The results obtained for $G(Q^2)$ are plotted in Fig. 4, where Q^2 varies inside the limits $Q^2 = 2 - 30 \text{ GeV}^2$.

As it has been emphasized above, the strong coupling G should be extracted at $q^2 = m_{B_c}^2$, i.e., at $Q^2 = -m_{B_c}^2$ where the SR method does not work. Therefore, we introduce the fit function $\mathcal{G}(Q^2)$ that at momenta $Q^2 > 0$ gives the same SR data, but can be extrapolated to the domain of negative Q^2 . For these purposes, we utilize the function

$$\mathcal{G}(Q^2, m^2) = \mathcal{G}^0 \exp \left[c^1 \frac{Q^2}{m^2} + c^2 \left(\frac{Q^2}{m^2} \right)^2 \right], \quad (31)$$

where \mathcal{G}^0 , c^1 , and c^2 are fitted constants. Then, having compared QCD output and Eq. (31), it is easy to find

$$\mathcal{G}^0 = 0.26 \text{ GeV}^{-1}, c^1 = 2.75, \text{ and } c^2 = -3.91. \quad (32)$$

This function is also shown in Fig. 4, where a nice agreement of $\mathcal{G}(Q^2)$ and QCD data is clear. For the strong coupling G , we find

$$G \equiv \mathcal{G}(-m_{B_c}^2) = (1.5 \pm 0.3) \times 10^{-1} \text{ GeV}^{-1}. \quad (33)$$

The width of the process $T_b \rightarrow \eta_b B_c^-$ is determined by the expression

$$\Gamma [T_b \rightarrow \eta_b B_c^-] = G^2 \frac{m_{\eta_b}^2 \lambda_0}{8\pi} \left(1 + \frac{\lambda_0^2}{m_{\eta_b}^2} \right), \quad (34)$$

where $\lambda_0 = \lambda(m, m_{\eta_b}, m_{B_c})$

$$\lambda(a, b, c) = \frac{\sqrt{a^4 + b^4 + c^4 - 2(a^2b^2 + a^2c^2 + b^2c^2)}}{2a}. \quad (35)$$

Then, we obtain

$$\Gamma [T_b \rightarrow \eta_b B_c^-] = (36.0 \pm 10.2) \text{ MeV}. \quad (36)$$

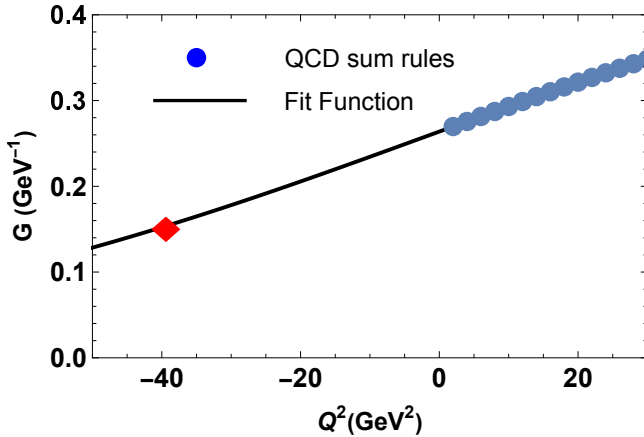


FIG. 4: The sum rule's data and fit function $\mathcal{G}(Q^2)$. The red diamond fixes the point $Q^2 = -m_{B_c}^2$ where G has been estimated.

IV. FULL WIDTH OF THE TETRAQUARK T_c

In this section, we compute the full width of the tetraquark T_c by considering the processes $T_c \rightarrow \eta_c B_c^+$ and $T_c \rightarrow J/\psi B_c^{*+}$. Both of them are kinematically allowed decay channels for this particle. In fact, thresholds for production of the final-state mesons $\eta_c B_c^+$ and $J/\psi B_c^{*+}$ are equal to 9259 MeV and 9435 MeV which are smaller than the mass $\tilde{m} = 9680$ MeV of the tetraquark T_c .

A. Decay $T_c \rightarrow \eta_c B_c^+$

Analysis of the process $T_c \rightarrow \eta_c B_c^+$ differ in some technical details from the investigation carried out in the previous section. Here, we explore the correlation function

$$\begin{aligned} \tilde{\Pi}(p, p') &= i^2 \int d^4x d^4y e^{ip'y} e^{-ipx} \langle 0 | \mathcal{T} \{ J^{B_c^+}(y) \\ &\quad \times J^{\eta_c}(0) \tilde{J}^\dagger(x) \} | 0 \rangle, \end{aligned} \quad (37)$$

where $J^{B_c^+}(x)$ and $J^{\eta_c}(x)$ are the interpolating currents for the mesons B_c^+ and η_c , respectively:

$$J^{B_c^+}(x) = \bar{b}_i(x) i\gamma_5 c_i(x), \quad J^{\eta_c}(x) = \bar{c}_j(x) i\gamma_5 c_j(x). \quad (38)$$

The matrix elements required to calculate the phenomenological side of SR are given the formulas

$$\begin{aligned} \langle 0 | J^{\eta_c} | \eta_c(q) \rangle &= \frac{f_{\eta_c} m_{\eta_c}^2}{2m_c}, \\ \langle 0 | J^{B_c^+} | B_c^+(p') \rangle &= \frac{f_{B_c} m_{B_c}^2}{m_b + m_c}, \end{aligned} \quad (39)$$

and

$$\langle \eta_c(q) B_c^+(p') | T_c(p) \rangle = g_1(q^2) p \cdot p'. \quad (40)$$

In the expressions above $m_{\eta_c} = (2984.1 \pm 0.4)$ MeV and $f_{\eta_c} = (421 \pm 35)$ MeV are the mass and decay constant of the charmonium η_c [38, 40].

The physical and QCD sides of the sum rule for the form factor $g_1(q^2)$ have the same analytical forms as ones provided in Sec. III. Therefore, we write down the SR for $g_1(q^2)$ which reads

$$\begin{aligned} g_1(q^2) &= \frac{4m_c(m_b + m_c)(q^2 - m_{\eta_c}^2)}{\Lambda f_{\eta_c} m_{\eta_c}^2 f_{B_c} m_{B_c}^2 (m^2 + m_{B_c}^2 - q^2)} \\ &\quad \times e^{m^2/M_1^2} e^{m_{B_c}^2/M_2^2} \Pi_1(\mathbf{M}^2, \mathbf{s}_0, q^2), \end{aligned} \quad (41)$$

where $\Pi_1(\mathbf{M}^2, \mathbf{s}_0, q^2)$ is the Borel-transformed and subtracted invariant amplitude extracted from the correlation function $\tilde{\Pi}^{\text{OPE}}(p, p')$.

In computations the parameters (M_1^2, s_0) in the T_c channel are varied within limits Eq. (20). The parameters (M_2^2, s'_0) in the B_c^+ channel are chosen inside the regions

$$M_2^2 \in [6.5, 7.5] \text{ GeV}^2, \quad s'_0 \in [45, 47] \text{ GeV}^2. \quad (42)$$

The form factor $g_1(Q^2)$ is computed at $Q^2 = 2-20$ MeV² (see, Fig. 5). The fit function $\mathcal{F}_1(Q^2, \tilde{m}^2)$ has the same functional form as the one in Eq. (31) but m^2 replaced by \tilde{m}^2 . This function in the case of the form factor $g_1(Q^2)$ has the parameters $\mathcal{F}_1^0 = 0.14 \text{ GeV}^{-1}$, $c_1^1 = 1.87$, and $c_1^2 = -3.58$ and is depicted in Fig. 5.

The strong coupling g_1 extracted at the mass shell $q^2 = -Q^2 = m_{\eta_c}^2$ amounts to

$$g_1 \equiv \mathcal{F}_1(-m_{\eta_c}^2) = (1.1 \pm 0.2) \times 10^{-1} \text{ GeV}^{-1}. \quad (43)$$

The width of the decay $T_c \rightarrow \eta_c B_c^+$ can be found by means of the formula

$$\Gamma [T_c \rightarrow \eta_c B_c^+] = g_1^2 \frac{m_{B_c}^2 \lambda_1}{8\pi} \left(1 + \frac{\lambda_1^2}{m_{B_c}^2} \right), \quad (44)$$

with λ_1 being equal to $\lambda(\tilde{m}, m_{B_c}, m_{\eta_c})$. Our result reads

$$\Gamma [T_c \rightarrow \eta_c B_c^+] = (26.9 \pm 6.9) \text{ MeV}. \quad (45)$$

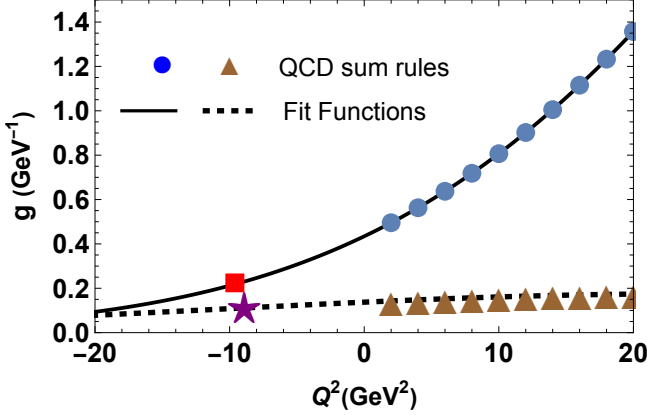


FIG. 5: Results of the sum rules computations and extrapolating functions $\mathcal{F}_1(Q^2)$ (dashed line) and $\mathcal{F}_2(Q^2)$ (solid line). The red star and square show positions $Q^2 = -m_{\eta_c}^2$ and $Q^2 = -m_{J/\psi}^2$, respectively.

B. Process $T_c \rightarrow J/\psi B_c^{*+}$

The second fall-apart mode of the tetraquark T_c is the decay to the pair of vector mesons $J/\psi B_c^{*+}$. To determine the strong coupling g_2 at the vertex $T_c J/\psi B_c^{*+}$, one has to evaluate the corresponding form factor $g_2(q^2)$, which can be extracted from the sum rule for this function. For this purpose, we analyze the correlation function

$$\begin{aligned} \Pi_{\mu\nu}(p, p') &= i^2 \int d^4x d^4y e^{ip'y} e^{-ipx} \langle 0 | \mathcal{T} \{ J_\mu^{B_c^*}(y) \\ &\quad \times J_\nu^{J/\psi}(0) \tilde{J}^\dagger(x) \} | 0 \rangle, \end{aligned} \quad (46)$$

where $J_\mu^{B_c^*}(x)$ and $J_\nu^{J/\psi}(x)$ are the interpolating currents of the vector mesons B_c^{*+} and J/ψ . These currents are introduced by means of the expressions

$$J_\mu^{B_c^*}(x) = \bar{b}_i(x) \gamma_\mu c_i(x), \quad J_\nu^{J/\psi}(x) = \bar{c}_j(x) \gamma_\nu c_j(x). \quad (47)$$

The phenomenological side of SR $\Pi_{\mu\nu}^{\text{Phys}}(p, p')$ is given by usual formula

$$\begin{aligned} \Pi_{\mu\nu}^{\text{Phys}}(p, p') &= \frac{\langle 0 | J_\mu^{B_c^*} | B_c^{*+}(p') \rangle \langle 0 | J_\nu^{J/\psi} | J/\psi(q) \rangle}{p'^2 - m_{B_c^*}^2} \frac{\langle T_c(p) | J^\dagger | 0 \rangle}{q^2 - m_{J/\psi}^2} \\ &\quad \times \langle B_c^{*+}(p') J/\psi(q) | T_c(p) \rangle \frac{\langle T_c(p) | J^\dagger | 0 \rangle}{p^2 - \tilde{m}^2} + \dots \end{aligned} \quad (48)$$

Here, $m_{J/\psi} = (3096.900 \pm 0.006) \text{ MeV}$ and $m_{B_c^*} = 6338 \text{ MeV}$ are the masses of the mesons $m_{J/\psi}$ and $m_{B_c^*}$, respectively. The first of them is the experimental value of $m_{J/\psi}$ [38], whereas $m_{B_c^*}$ —the theoretical prediction [41].

The correlator $\Pi_{\mu\nu}^{\text{Phys}}$ can be simplified by employing the matrix elements

$$\begin{aligned} \langle 0 | J_\mu^{B_c^*} | B_c^{*+}(p') \rangle &= f_{B_c^*} m_{B_c^*} \varepsilon'_\mu, \\ \langle 0 | J_\nu^{J/\psi} | J/\psi(q) \rangle &= f_{J/\psi} m_{J/\psi} \varepsilon_\nu, \end{aligned} \quad (49)$$

and

$$\begin{aligned} \langle B_c^{*+}(p') J/\psi(q) | T_c(p) \rangle &= g_2(q^2) [(q \cdot p')(\varepsilon'^* \cdot \varepsilon^*) \\ &\quad - (q \cdot \varepsilon'^*)(p' \cdot \varepsilon^*)]. \end{aligned} \quad (50)$$

In Eq. (49) $f_{J/\psi} = (411 \pm 7) \text{ MeV}$ and $f_{B_c^*} = 471 \text{ MeV}$ are the decay constants of the mesons J/ψ and B_c^{*+} , respectively [42, 43].

Then, for $\Pi_{\mu\nu}^{\text{Phys}}(p, p')$ we get

$$\begin{aligned} \Pi_{\mu\nu}^{\text{Phys}}(p, p') &= \frac{g_2(q^2) \tilde{\Lambda} f_{B_c^*} m_{B_c^*} f_{J/\psi} m_{J/\psi}}{(p^2 - \tilde{m}^2)(p'^2 - m_{B_c^*}^2)(q^2 - m_{J/\psi}^2)} \\ &\quad \times \left[\frac{g_{\mu\nu}(m^2 - m_{B_c^*}^2 - q^2)}{2} - q_\mu p'_\nu + \text{other structures} \right]. \end{aligned} \quad (51)$$

The correlation function $\Pi_{\mu\nu}(p, p')$ expressed in terms of the heavy quark propagators is

$$\begin{aligned} \Pi_{\mu\nu}^{\text{OPE}}(p, p') &= 2 \int d^4x d^4y e^{ip'y} e^{-ipx} \{ \text{Tr} [\gamma_\nu S_c^{ja}(-x) \\ &\quad \times \gamma_\alpha \tilde{S}_c^{ib}(y-x) \gamma_\mu \tilde{S}_b^{ai}(x-y) \gamma^\alpha S_c^{bj}(x)] \\ &\quad - \text{Tr} [\gamma_\nu S_b^{ja}(-x) \gamma_\alpha \tilde{S}_c^{ib}(y-x) \gamma_\mu \tilde{S}_b^{bi}(x-y) \gamma^\alpha S_c^{aj}(x)] \}. \end{aligned} \quad (52)$$

To derive SR for the form factor $g_2(q^2)$, we utilize the invariant amplitudes $\Pi_2^{\text{Phys}}(p^2, p'^2, q^2)$ and $\Pi_2^{\text{OPE}}(p^2, p'^2, q^2)$ which correspond to terms proportional to $-q_\mu p'_\nu$ in Eqs. (51) and (52). As a result, we find for $g_2(q^2)$

$$\begin{aligned} g_2(q^2) &= \frac{(q^2 - m_{J/\psi}^2)}{\tilde{\Lambda} f_{B_c^*} m_{B_c^*} f_{J/\psi} m_{J/\psi}} \\ &\quad \times e^{m^2/M_1^2} e^{m_{B_c^*}^2/M_2^2} \Pi_2(\mathbf{M}^2, \mathbf{s}_0, q^2). \end{aligned} \quad (53)$$

Operations to calculate the strong coupling g_2 of particles at the vertex $T_c J/\psi B_c^{*+}$ have been described above, therefore, we provide relevant information in a brief form. Thus, the form factor $g_2(Q^2)$ is computed at $Q^2 = 2 - 20 \text{ MeV}^2$. In calculations the parameters (M_1^2, s_0) in the T_c channel are chosen in accordance with Eq. (20). In the B_c^{*+} channel the parameters (M_2^2, s'_0) change in the regions

$$M_2^2 \in [6.5, 7.5] \text{ GeV}^2, \quad s'_0 \in [50, 51] \text{ GeV}^2. \quad (54)$$

The extrapolating function $\mathcal{F}_2(Q^2, \tilde{m}^2)$ has the following parameters: $\mathcal{F}_2^0 = 0.43 \text{ GeV}^{-1}$, $c_2^1 = 6.26$, and $c_2^2 = -4.33$. Then, the coupling g_2 is equal to

$$g_2 \equiv \mathcal{F}_2(-m_{J/\psi}^2) = (2.2 \pm 0.4) \times 10^{-1} \text{ GeV}^{-1}. \quad (55)$$

The width of the decay $T_c \rightarrow J/\psi B_c^{*+}$ is determined by employing the expression

$$\Gamma [T_c \rightarrow J/\psi B_c^{*+}] = g_2^2 \frac{\lambda_2^3}{4\pi} \left(1 + \frac{3m_{B_c^*}^2 m_{J/\psi}^2}{2\tilde{m}^2 \lambda_2^2} \right), \quad (56)$$

where λ_2 is $\lambda(\tilde{m}, m_{B_c^*}, m_{J/\psi})$. We find

$$\Gamma [T_c \rightarrow J/\psi B_c^{*+}] = (27.8 \pm 7.1) \text{ MeV}. \quad (57)$$

The full width of the tetraquark T_c saturated by these two decay channels is

$$\Gamma [T_c] = (54.7 \pm 9.9) \text{ MeV}. \quad (58)$$

V. CONCLUSIONS

In the current paper, we have calculated the masses and widths of the scalar tetraquarks $T_b = bb\bar{b}\bar{c}$ and $T_c = cc\bar{c}\bar{b}$ in the context of QCD sum rule method. These particles have been modeled as diquark-antidiquark systems made of the axial-vector diquarks and antidiquarks. Their masses have been evaluated using the two-point sum rule approach, whereas to estimate the widths of these tetraquarks we have invoking techniques of the three-point sum rule approach. Here, we have considered only the dissociations of T_b and T_c to conventional mesons, which are their dominant decay channels. There are also modes generated by annihilations of $b\bar{b}$ and $c\bar{c}$ quarks inside of T_b and T_c . But, the partial widths of these processes, as usual, are smaller than that of the dominant channels and have not been taken into account in this article.

The tetraquarks T_b and T_c have different parameters and features. Thus, T_b and T_c bear a unit of negative and positive electric charge, respectively. The gap between the masses of these particles is approximately equal to the mass difference of corresponding constituent quarks. The structure T_b with the width 36.0 MeV is narrower than the tetraquark T_c . The reason is that the mass m of

T_b exceeds only $\eta_b B_c^-$ threshold, whereas \tilde{m} overshoots kinematical limits for productions of $\eta_c B_c^+$ and $J/\psi B_c^{*+}$ mesons.

In our previous works, we performed rather detailed investigation of the fully heavy tetraquarks. With related information at hand, it is instructive to compare the masses of the fully heavy scalar tetraquarks containing different number of valence $b(\bar{b})$ quarks and analyze their stability against dissociation to ordinary mesons. The four-quark meson containing one \bar{b} quark has been explored in the present paper. Its mass exceeds 421 MeV the lowest $\eta_c B_c^+$ threshold which makes possible decays to $\eta_c B_c^+$ and $J/\psi B_c^{*+}$ pairs.

There are two classes of particles with two constituent $b(\bar{b})$ quarks. The first class includes states with bb diquarks or $\bar{b}\bar{b}$ antidiquarks, whereas the hidden charm-bottom tetraquarks form the second type of such particles: They have the $bc\bar{b}\bar{c}$ structures. The scalar exotic meson $bb\bar{c}\bar{c}$ was explored in our paper [10], in which its mass was found equal to 12715 MeV, i.e., approximately 166 MeV above the $2B_c^-$ mesons' mass. The scalar tetraquark $bc\bar{b}\bar{c}$ with the mass 12697 MeV is 166 MeV heavier than the lowest $B_c^- B_c^+$ final-state [24].

The scalar diquark-antidiquark state $T_b = bb\bar{b}\bar{c}$ have been explored in the present work and found only 25 MeV exceeding the $\eta_b B_c^-$ mass limit. Finally, the scalar tetraquark $X_{4b} = b\bar{b}b\bar{b}$ is below the $\eta_b \eta_b$ threshold and stable against decays to these mesons [4]. But X_{4b} can still transform to ordinary particles through strong interaction due to annihilation of $b\bar{b}$ quarks and production of $B_q \bar{B}_q$ and $B_q^* \bar{B}_q^*$ pairs [44].

As is seen, stability of the fully heavy tetraquarks against fall-apart processes and their widths depend on a number of valence $b(\bar{b})$ quarks. Our analysis of all-heavy exotic mesons and collected theoretical information on their masses and widths can be used in analyses of future experimental data.

ACKNOWLEDGEMENTS

K. Azizi thanks Iran national science foundation (INSF) for the partial financial support provided under the elites Grant No. 4037888. He is also grateful to the CERN-TH department for their support and warm hospitality.

-
- [1] R. Aaij *et al.* (LHCb Collaboration), *Sci. Bull.* **65**, 1983 (2020).
 - [2] E. Bouhova-Thacker (ATLAS Collaboration), *PoS ICHEP2022*, 806 (2022).
 - [3] A. Hayrapetyan, *et al.* (CMS Collaboration) *Phys. Rev. Lett.* **132**, 111901 (2024).
 - [4] S. S. Agaev, K. Azizi, B. Barsbay, and H. Sundu, *Phys. Lett. B* **844**, 138089 (2023).
 - [5] S. S. Agaev, K. Azizi, B. Barsbay and H. Sundu, *Eur. Phys. J. Plus* **138**, 935 (2023).
 - [6] S. S. Agaev, K. Azizi, B. Barsbay and H. Sundu, *Nucl. Phys. A* **844**, 122768 (2024).
 - [7] S. S. Agaev, K. Azizi, B. Barsbay and H. Sundu, *Eur. Phys. J. C* **83**, 994 (2023).
 - [8] C. Becchi, A. Giachino, L. Maiani, and E. Santopinto, *Phys. Lett. B* **806**, 135495 (2020).

- [9] C. Becchi, A. Giachino, L. Maiani, and E. Santopinto, Phys. Lett. B **811**, 135952 (2020).
- [10] S. S. Agaev, K. Azizi, B. Barsbay, and H. Sundu, J. Phys. G **51**, 115001 (2024).
- [11] S. S. Agaev, K. Azizi, and H. Sundu, Phys. Lett. B **851**, 138562 (2024).
- [12] S. S. Agaev, K. Azizi, and H. Sundu, Phys. Lett. B **856**, 138886 (2024).
- [13] F. Carvalho, E. R. Cazaroto, V. P. Gonsalves, and F. S. Navarra, Phys. Rev. D **93**, 034004 (2016).
- [14] L. M. Abreu, F. Carvalho, J. V. C. Cerquera, and V. P. Goncalves, Eur. Phys. J. C **84**, 470 (2024).
- [15] R. N. Faustov, V. O. Galkin, and E. M. Savchenko, Symmetry **14**, 2504 (2022).
- [16] J. Wu, Y. R. Liu, K. Chen, X. Liu, and S. L. Zhu, Phys. Rev. D **97**, 094015 (2018).
- [17] M. S. Liu, Q. F. Lü, X. H. Zhang, and Q. Zhao, Phys. Rev. D **100**, 016006 (2019).
- [18] X. Chen, Phys. Rev. D **100**, 094009 (2019).
- [19] M. A. Bedolla, J. Ferretti, C. D. Roberts, and E. Santopinto Eur. Phys. J. C **80**, 1004 (2020).
- [20] M. C. Gordillo, F. De Soto, and J. Segovia Phys. Rev. D **102**, 114007 (2020).
- [21] X. Z. Weng, X. L. Chen, W. Z. Deng, and S. L. Zhu Phys. Rev. D **103**, 034001 (2021).
- [22] Z. H. Yang, Q. N. Wang, W. Chen, and H. X. Chen Phys. Rev. D **104**, 014003 (2021).
- [23] J. Hoffer, G. Eichmann, C. S. Fischer, Phys. Rev. D **109**, 074025 (2024).
- [24] S. S. Agaev, K. Azizi, and H. Sundu, Phys. Lett. B **858**, 139042 (2024).
- [25] S. S. Agaev, K. Azizi, and H. Sundu, arXiv:2410.00575 [hep-ph].
- [26] S. S. Agaev, K. Azizi, and H. Sundu, arXiv:2410.22439 [hep-ph].
- [27] C. Deng, H. Chen, and J. Ping, Phys. Rev. D **103**, 014001 (2021).
- [28] G. Yang, J. Ping, and J. Segovia Phys. Rev. D **104**, 014006 (2021).
- [29] H. Mutuk, Phys. Lett. B **834**, 137404 (2022).
- [30] J. Zhang, J. B. Wang, G. Ji, C. S. An, C. R. Deng, and J. J. Xie, Eur. Phys. J. C **82**, 1126 (2022).
- [31] V. O. Galkin, and E. M. Savchenko, Eur. Phys. J. A **60**, 96 (2024).
- [32] M. A. Shifman, A. I. Vainshtein and V. I. Zakharov, Nucl. Phys. B **147**, 385 (1979).
- [33] M. A. Shifman, A. I. Vainshtein and V. I. Zakharov, Nucl. Phys. B **147**, 448 (1979).
- [34] M. L. Du, W. Chen, X. L. Chen, and S. L. Zhu, Phys. Rev. D **87**, 014003 (2013).
- [35] R. L. Jaffe, Phys. Rept. **409**, 1 (2005).
- [36] R. M. Albuquerque, J. M. Dias, K. P. Khemchandani, A. Martinez Torres, F. S. Navarra, M. Nielsen and C. M. Zanetti, J. Phys. G **46**, 093002 (2019).
- [37] S. S. Agaev, K. Azizi and H. Sundu, Turk. J. Phys. **44**, 95 (2020).
- [38] R. L. Workman *et al.* [Particle Data Group], Prog. Theor. Exp. Phys. **2022**, 083C01 (2022).
- [39] Z. G. Wang, Chin. Phys. C **48**, 103104 (2024).
- [40] E. V. Veliev, K. Azizi, H. Sundu, and N. Aksit, J. Phys. G **39**, 015002 (2012).
- [41] S. Godfrey, Phys. Rev. D **70**, 054017 (2004).
- [42] O. Lakhina, and E. S. Swanson, Phys. Rev. D **74**, 014012 (2006).
- [43] E. J. Eichten, and C. Quigg, Phys. Rev. D **99**, 054025 (2019).
- [44] S. S. Agaev, K. Azizi, B. Barsbay, and H. Sundu, Phys. Rev. D **109**, 014006 (2024).